ISSN PRINT 2319 1775 Online 2320 7876

 UGC CARE Listed (Group -I) Journal Volume 11, S Iss 2, 2022

The Diurnal Variation Characteristics of Latent Heat Flux under Different Underlying Surfaces and Analysis of Its Drivers

Dr. Rajendra Bapurao Vhatkar[1], Dr. Vishwajeet S.Goswami[2], Prof. Manishkumar Jaiswal[3]

[1]*Asst Professor, Dept. of Mathematics, S.N College of Arts & Commerce, Thane, Maharashtra.*

[2]*Asst. Professor, Dept. of Mathematics, UIS. Chandigarh University*

[3]*Assistant Professor, Department of Mathematics, Shri Chinai College of Commerce & Economics, Mumbai, Maharashtra.*

Abstract : Monitoring the Latent Heat Flow is crucial for managing water resources and determining the crop water demand because it is a crucial part of the hydrological cycle and surface water heat transfer. The Heihe River Basin's distinctive topography guarantees improved variable control in LE analysis. In this work, the time series analysis and statistics of LE under various underlying surface conditions in the summer were carried out, and the regression components were looked at, using the eddy correlation observation data from the Heihe River Basin.The results show that when the underlying surface types are significantly different, there are discernible differences in the daily distribution of LE, the daily fluctuation trend of LE, and the influencing factors. The range of LE's diurnal distribution in the desert, Gobi, and dunes is 50 to 100 W/m2.Vegetable fields, cornfields, and marshes had a diurnal LE distribution that was roughly 55% concentrated between 50 and 100 W/m2. The two main elements influencing latent heat flux are temperature and carbon dioxide content (CO2). Stepwise regression analysis is used to further analyse temperature and CO2 levels, and numerous regression models are created. In terms of correlation and confidence, the outcomes outperform single factor fitting and are better able to reflect the interplay between temperature and CO2 on LE.

Keywords :- Eddy correlation, latent heat flux, the underlying surface, the weather, and an area with sparse vegetation

1. Introduction

Latent heat flux , which is evapotranspiration's energy expression, plays a key role in the hydrologic cycle, hydrologic prediction, and activities involving the transfer of heat from surface water. [1–5]

ISSN PRINT 2319 1775 Online 2320 7876

 UGC CARE Listed (Group -I) Journal Volume 11, S Iss 2, 2022

Latent heat of evapotranspiration is one of the key mechanisms controlling the energy and water exchange between the hydrosphere, atmosphere, and biosphere [6,7]. It is a crucial component of the hydrological cycle because it reflects the environment's highest water demand and helps to keep the water balance [8,9]. Evapotranspiration reflects the water needs of crops, however it is challenging to quantify evapotranspiration precisely. The LE can better depict evapotranspiration. From a meteorological and environmental perspective, the climate and environmental factors that affect LE typically include net radiation, relative humidity, air temperature, and leaf area index.

Numerous academics and researchers have studied and analysed the response relationship between LE and its drivers on the space-time scale, but the results are not always consistent, particularly when categorising the sensitivity of meteorological parameters [10–12].It suggests that there is some one-sidedness in the way temperature, environment, and other variables are controlled when examining the interaction between drivers and LE in terms of responsiveness. The analysis results from past study were usually spatially dependent and difficult to build a sound inquiry since there was typically only one underlying surface or a large spatial difference between many underlying surfaces.The estimation and measurement methods for LE have long been a hot topic among academics.Numerous methods are used to assess evapotranspiration, including the owen ratio energy balance approach, remote sensing, in situ measurement, hydrologic, and eddy correlation methods [13–19].Under challenging geomorphological circumstances, the accuracy of the Bowen ratio-energy balance method is constrained. The hydrology approach, which is founded on the concept of water balance, is used to calculate the total evapotranspiration in the study area. The method has drawbacks, such as a long temporal scale (water balance approach) or a brief spatial scale (vaporation method) [20,21].Although remote sensing can be used for extensive long-term observations, it cannot be continuous because of the short transit time and limited operating cycle of satellites. The circumstances that apply, the theoretical underpinnings, and the measuring range of various approaches vary. Eddy correlation can quickly gather a lot of data on evapotranspiration and environmental change since fewer theoretical presumptions, high precision, rapid measurement, and great temporal resolution are some of its benefits. [22].The technique offers a direct confirmation for the currently used soil-

ISSN PRINT 2319 1775 Online 2320 7876

 UGC CARE Listed (Group -I) Journal Volume 11, S Iss 2, 2022

vegetation-atmosphere material-energy exchange model. The "Joint Experiment on Integrated Remote Sensing Observation of Eco-Hydrological Processes in the Heihe River Basin" (EC) system, which was developed [23], is used in the study. Variable control is ensured throughout LE analysis thanks to the Heihe River Basin's diverse landscape, which includes sand dunes, the Gobi Desert, vegetable and maize crops, and deserts.The middle reaches of the Heihe River's typical desert oasis landform are the subject of this study and is based on the EC system observation data of the "Integrated Remote Sensing Observation Joint Experiment of Eco-Hydrological Processes in the Heihe River Basin" [14] and based on factors including correlation analysis, LE daily variation curve, and LE daily frequency distribution, among others. The properties of latent heat flux and the response relationship of its influencing components are explored while taking into account spatiotemporal variation and land cover type.

2. Substantials and Acting Methods

Research Area of Study

The research area is located in Zhangye City, Gansu Province, which is the central oasis in the middle reaches of the Heihe River Basin (HRB) (100.104-100.853 E, 38.549-39.399 N).With an average height of 1474 metres, the middle temperate zone has semi-arid and arid weather.In July, the average monthly high temperature is 29.3 degrees Celsius, while January has an average monthly low temperature of 16.2 degrees Celsius.July has 9.4 days of average monthly precipitation, 130.44 mm of average annual precipitation, and 51.6 days of average annual precipitation.With an average yearly evaporation of 2000–3500 mm and a large difference in temperature between day and night, the region sees significant evaporation.

Six stations were chosen for this article. In Zhangye city, Gansu province's Daman irrigation district, is where you'll find the Daman superstation. While the undersides of encryption stations 1 and 12 are both vegetable fields and cornfields, respectively, the Huazhaizi station has a typical desert subsurface with sparse red and pearl sand sprouting on the surface.Due to the Bajitan station's primary coarse sand and gravel surface, a lack of water, and a paucity of plants, only a few drought-tolerant species, like tamarisk and camel thorn, may grow there. The Shenshawo station is a desert area mostly covered in sand with unusual plants and dry air, in contrast to the Wetland station where the underlying surface is a wetland with adequate wetness and rich

ISSN PRINT 2319 1775 Online 2320 7876

 UGC CARE Listed (Group -I) Journal Volume 11, S Iss 2, 2022

vegetation.The Heihe Hydrological Remote Sensing Experiment's subsite stations of the Daman Super Station are fields of vegetables and maize, where the information for these stations was gathered. These websites are thorough, educational, and excellent for research. The precise statistics and site distribution in the study area are shown in Table 1 and Figure 1. The land cover of the Heihe River Basin is shown in Figure 2 [24].

Table 1. Site name and study topic-related details

Name of Site	Underlay Surface name	Altitude	Data in and out time
station 1	Vegetable ground	1552.8 5	June–31 August
station 12	Cornfifield	1559.3 1	June–31 August 31
Shenshawo station	Dune	1562.6	1 June–31 August (data unavailable on August 2)
	Gobi	1731.0	
jitan station	Desert	1549.4 2	7 June – 31 August
	Wetland	1460.0	June–30 August
Huazhaizi station			26 June to 30 August
Wetland station			

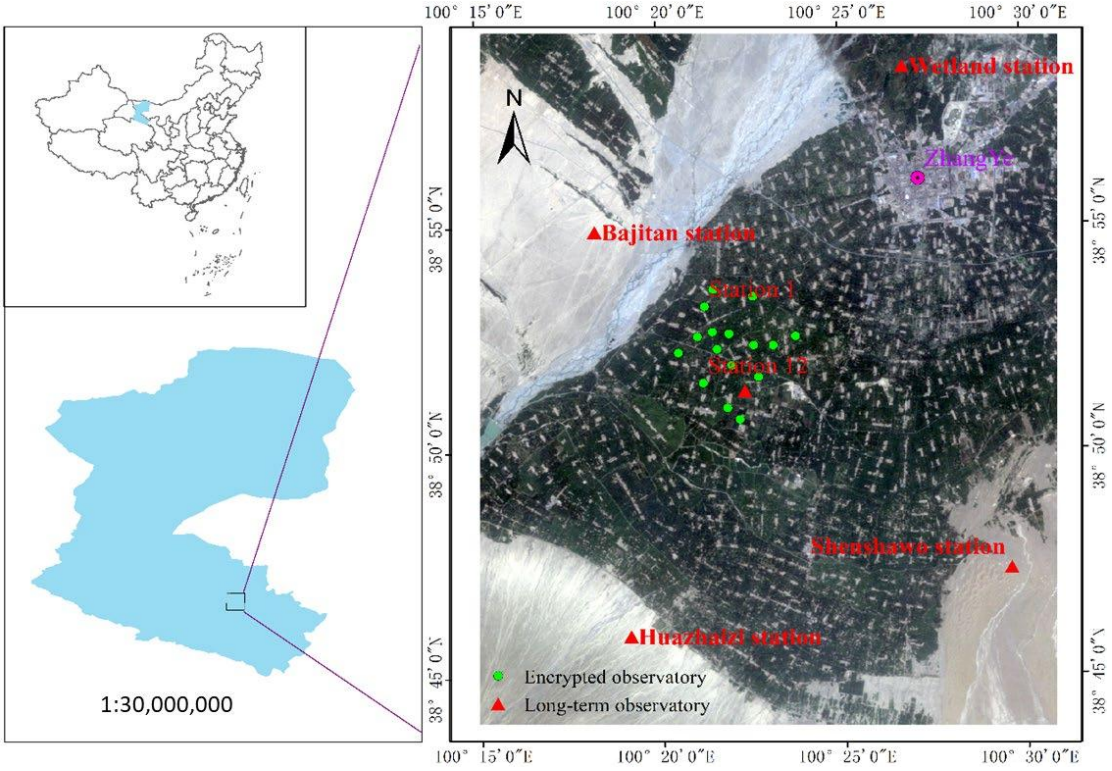

ISSN PRINT 2319 1775 Online 2320 7876

 UGC CARE Listed (Group -I) Journal Volume 11, S Iss 2, 2022

Figure 1. Map of the research area's locations and site dispersal.

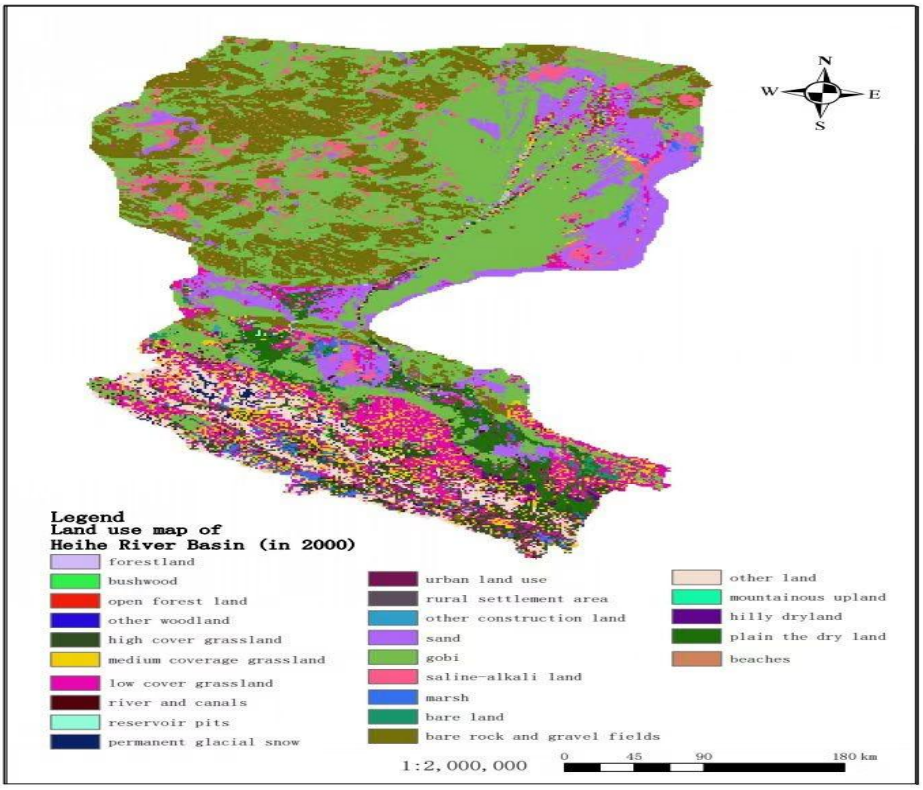

Figure 2. Heihe River Basin land cover map.

2.2. Tool and Trial Content

An image spectrometer, a charge-coupled device (CCD), a light detection and ranging (lidar) system, a multi-angle thermal infrared camera, a microwave radiometer, and a light detection and range system were all employed in the experiment.The standard automatic meteorological station (AMS) measures the soil heat flux, soil moisture and temperature profiles, air pressure, wind direction and speed, air temperature, and radiation throughout the entire HRB.The superstation was outfitted with an EC system, a Bowen ration energy balancing device, a LAS (long aperture scintillometer), and a lysimeter to monitor fluxes at various scales.The land surface temperature (LST), photosynthetically active radiation (PAR), and standard station data are all also measured by superstations. The instrument is thoroughly introduced in Li's paper [25,26].

2.3. Research Data

ISSN PRINT 2319 1775 Online 2320 7876

 UGC CARE Listed (Group -I) Journal Volume 11, S Iss 2, 2022

The data required for this paper come from the "Joint Telemetry Experimental Study in the Heihe River Basin," also known as "HiWATER [23,26,27], this combines an experiment with the observation of ecohydrological processes using remote sensing in the Heihe River Basin.In addition to two encrypted stations 1 and 12 in the Daman irrigation region (a vegetable field and a cornfield, respectively), the following will make use of the Gobi, desert, dune, and wetland stations.Bajitan, Huazhaizi, Shenshawo, wetland station in the middle reaches of the Heihe River, and wetland station made up the total of six stations chosen for this investigation.The horizontal wind velocity, air temperature, water vapour density, carbon dioxide concentration, and latent heat flux EC observation data were selected and obtained via the Heihe Plan Data Management Centre Network (http://westdc.westgis.ac.cn, accessed on: 1 September 2022).Although there were gaps in the data for the weeks prior to June 25 at the wetland station and August 2 at the Bajitan Station, the data interval on average was 30 minutes. The start and end times of the study area locations and data are shown in Table 1.

2.4. Data Process

The EC observations have a minor number of missing values. The early and late time periods are where the majority of the missing portion is located and the interpolation data is mostly LE. The analysis is unaffected by the lack of a clear LE trend over these two time periods. The addition of linear interpolation to the data. Stepwise regression analyses presented screening findings in descending order and took taking the involvement of independent factors into consideration. Since model identification merely needs optimising the coefficients of each input, it is frequently used [28]. The AIC (Akaike information criterion) criterion is then applied to achieve automatic parameter optimisation.

Stepwise regression techniques and correlation coefficients (R) must be utilised to analyse LE and its drivers in this work.The introductions that follow are connected: The R has been commonly employed to quantify the average disparity between models, despite the fact that they are oversensitive to high extreme values (outliers) [29,30].

R will be defined as

$$R = \frac{n\sum i=1\ (Q0(i) - Q0)(Qf(i) - Qf)\ s}{Sq\,(n\sum i=1\ (Q0(i) - Q0)2) * Sq\,(\,n\sum i=1\ (Qf(i) - Qf)2)}$$

ISSN PRINT 2319 1775 Online 2320 7876

 UGC CARE Listed (Group -I) Journal Volume 11, S Iss 2, 2022

The information-theoretic approaches provide the foundation of Akaike's information criterion (AIC) [31]. It serves as a benchmark for judging the accuracy of statistical model fitting and the complexity of statistical models. The complexity of the model tends to rise as the amount of data used in model training increases. At the same time, it is challenging to prevent overfitting issues. Methods like AIC and BIC (Bayesian Information Criterion) are frequently used to prevent over-fitting of the model. Given a large sample size, the BIC method yields a more desirable result because its penalty term is larger than that of the AIC method [32]. To prevent overfitting, we should prioritise models with the lowest AIC values when using AIC to assess model fit [33].

Generally A/C expressed as

$AIC = 2k - 2\ln(L)$ …….. (a)

L is the likelihood function, and k is the number of parameters.

The error of the model is subject to a separate normal distribution:

$AIC = 2k + n\ln(RSS/n)$ ……(b)

where n is the number of observations, and RSS (Residual Sum of Squares) denotes the total of the residuals.

Multiple regression analysis usually involves a large number of effect factors, therefore computing the full set of parameters can be highly expensive [34].

Stepwise regression is a trustworthy method [35]

Following the quadratic response surface model, the stepwise regression model is shown as

$y(x) = a0 + \sum_{i=1}^{n} aixi + \sum_{i=1}^{n} aiixi\text{^}2 + \sum_{j<1}^{n} ajixjxi$

The stepwise regression approach adds the significant independent variables into the regression equation in the order of the independent variables in the model.

Reexamining the significance level test at the predetermined F or AIC level and removing variables that are not significantly impacted by the dependent variable until the variables are unable to improve the model by reintroducing the independent variables results in the completion of the regression process and the best regression equation [34,35].Equation (4) states that factor interactions as well as linear or nonlinear correlations among factors may be the subjects of stepwise regression. A flowchart of the calculations is shown in Figure 3.

3. Results

3.1. Analysis of the Trend in LE Variation for Various Underlying Surface Types

ISSN PRINT 2319 1775 Online 2320 7876

 UGC CARE Listed (Group -I) Journal Volume 11, S Iss 2, 2022

Using LE data from the months of June, July, and August of 2012, a time series visual based on numerous underlying surface types was produced.

Figure 3 demonstrates that LE has a comparable pattern over time and that the current underlying surface conditions (soil moisture content and vegetation coverage) are comparable.These elements suggest that the current underlying surface conditions are likely to persist when combined with the weather data for Zhangye city in June, July, and August 2012. Additional information on the LE trend line's fluctuation is obtained, which is roughly consistent with changes in the weather from sunny to rainy.

In order to further evaluate the characteristics and distribution rules of LE days with sunny days used as a control variable, station data (vertical line markers) with weather conditions as sunny days for three months were selected.

Using sunny days as a control condition and based on several sites, we selected the 9-day LE data for the dates of 8 June, 19 June, 29 June, 9 July, 13 July, 31 July, 2 August, 21 August, and 27 August 2012.The nine days of the LE intraday frequency distribution histogram were then mapped. Additionally offered are statistics for LE days.As demonstrated in Figure 4 and Table 2, each site's peak value and standard deviation are notably different, and this variation is directly related to the type of underlying surface.The LE maximum for vegetated land was 661.3 W/m2, whereas the LE minimum for dunes was 201.2 W/m2. The LE standard deviation for cornfield is 180.8 W/m2, while the LE standard deviation for dunes is 39.3 W/m2.While the distribution of LE values in the Gobi, sand, and desert is largely dispersed and gradual, it is relatively concentrated and steep in vegetable fields, cornfields, and wetland.

The kurtosis can show how steeply and slowly the pattern is spread, and the standard deviation can show how dispersed the study object is.

The cumulative values for the Gobi, dune, and desert on the 50-100 W/m2 interval are 92.4%, 89.5%, and 94.1%, respectively. The cumulative values for the vegetable land, corn land, and wetland on the 50-100 W/m2 interval are 53.8%, 54%, and 57.7%, respectively.

Even though the underlying surface features of each site differ, a careful analysis of the aforementioned data allows us to approximately divide each site into two groups: dry (Gobi, dune, desert) and moist (vegetable, maize, and wetland).The LE value of the underlying surface is concentrated between 50 and 100 W/m2 in a dry atmosphere.

ISSN PRINT 2319 1775 Online 2320 7876

 UGC CARE Listed (Group -I) Journal Volume 11, S Iss 2, 2022

Under the moist circumstances of the underlying surface, the LE value is concentrated between 50 and 100 W/m2, but with a significant degree of dispersion; 42.2 to 46.2% of the LE value is scattered over 100 W/m2.Evapotranspiration requires three driving factors: an energy source, sufficient water for the vegetation, hot summer temperatures, and surface temperature.While the amount of water vapour travelling upward diffusion and evaporation increases, a relatively wet environment, vegetation cover in a dry environment, a lack of soil moisture, plant transpiration, and soil evaporation all contribute to an insufficient water supply [36, 37]. The study's findings [38] support the idea that a wetland ecosystem has a far wider range of variation in latent heat flux than a dryland environment.

Table 2. LE statistical results of 9 days were synthesized under different types of underlying surfaces

Site Name	Standard Deviation /(W/m2)	Average /(W/m2)	Maximum /(W/m2)	Minimum /(W/m2)	Kurtosis Partial	Degrees
station 1	162.35	154.12	661.32	−67.13	−0.28	0.91
station 12	180.83	164.91	627.27	−75.64	−0.69	0.23
Bajitan station	40.98	29.6	205.03	−56.5	2.99	1.6
Huazhaizi station	56.45	46.26	292.91	−71.79	2.34	1.55
Shenshawo station	39.28	29.90	201.23	−95.75	2.68	1.11
Wetland station	168.83	152.44	636.53	−23.52	−0.4	0.13

3.2. An analysis of the LE's intraday variation trend on several underlying surfaces

For numerous locations, the variance trend of the same site during LE days at various times was examined.Figure 5 shows that the variation trend across several sites was mostly stable within LE days.Bright days and less data loss, which are based on the climatic conditions at various points in June, July, and August, are the basis for the

ISSN PRINT 2319 1775 Online 2320 7876

 UGC CARE Listed (Group -I) Journal Volume 11, S Iss 2, 2022

lack of EC observation data.The usual days of 29 June, 13 July, and 27 August were used in order to further explore the variation trend of LE intraday at various locations on the same time scale (see Figure 6 for additional details). On June 29, the LE intraday trend lines at all stations were significantly influenced by the underlying surface. At 9:30, there were intermittent changes in each station's LE intraday trend lines. Now, the marshes, cornfields, and vegetable farms' LE intraday trend lines were increasing.Around noon, the value of the vegetable and cornfields reached its peak, following which the upward trend slowed. The minimum value was discernible at 12:30 and 13:00, respectively. The cornfield and vegetable area's broad horizontal vibration saw many peaks between 12:00 and 15:00. The intraday trend line for the wetland reached its peak at 13:00 and thereafter showed a tendency to oscillate and decline that was somewhat different from the trend lines for the cornfield and wetland. Throughout LE days, the same area was checked out at various times. Figure 5 shows that the variation trend across several sites was mostly stable within LE days. Bright days and less data loss, which are based on the climatic conditions at various points in June, July, and August, are the basis for the lack of EC observation data.The variance trend of LE intraday at various locations was further examined on typical days like June 29, July 13, and August 27.The LE intraday trend line patterns on July 13 varied slightly between the two sites.

Between 14:00 and 15:00, the average LE value in wetlands, vegetable fields, and cornfields achieved its peak value. The peak form was a single peak, the highest level in three months.

On the other hand, the average LE value for the dune, desert, and Gobi was at its lowest point in three months, and the trend line has a history of stability and low volatility. Only 33.69 W/m2, 56.16 W/m2, and 34.83 W/m2 were the daily average LE values.

The diurnal fluctuation trend of LE at all locations on August 27 was nearly the same as it was on July 13 [40].Vegetable land peak values dropped sharply from July to the lowest level in three months, followed by maize land and wetland peak values [41].

After carefully analysing the three days of data, it is evident that while there is little variation between each site's daily LE trend line on June 29, July 13, and August 27, there is a significant difference between the daily LE trend of different sites when compared to the other sites.

ISSN PRINT 2319 1775 Online 2320 7876

 UGC CARE Listed (Group -I) Journal Volume 11, S Iss 2, 2022

3.3. Analysis of LE Drivers for Various Types of Underlying Surface

In various underlying surface types, this section examines the link between LE and its driving components. According to Table 3 and the correlation coefficient data of each driving factor, the LE of this site is significantly correlated with the two driving factors: temperature and CO2.According to the ranking of stations in Table 2, the correlation coefficients between temperature and LE were 0.72, 0.70, 0.31, 0.45, 0.39, and 0.68, respectively, and the link was very significant (p 0.01). The link between CO2 and LE was very significant (p 0.01) and had correlation values of 0.64, 0.64, 0.28, 0.34, 0.18, and 0.65, respectively.The link between water vapour density and LE was either positive or negative depending on the area.Figure 7's regression curve demonstrates that when soil moisture levels are high, LE and temperature grow exponentially and at a far faster rate than when soil moisture levels are low. The temperature patterns of LE and CO2 are comparable [42].

The Shenshawo station, which forms the base of the sand dune, is where the increase of LE with CO2 occurs. This increase has a turning point that is obviously different from the monotonous change of CO2 on the LE.In this work, stepwise regression analysis was used to create multiple regression equations using two drivers (air temperature and CO2) that had strong association at each location.

3.4. Defificiencies and Discussions

Using EC observation data from the HiWATER test, this study analysed and examined the characteristics of evapotranspiration and the effects of various parameters on LE fluxes under diverse underlying surface types.The distribution and intradermal variation trend of latent heat flux change depending on the underlying surface characteristics of dry (dune, desert, Gobi) and wet (vegetable land, maize land, wetland), with vegetation cover having a stronger influence on latent heat flux.

Due to the short observation period of this experiment, the associated hydrological yearly frequency is singular, which may be impacted by the uneven distribution of rainfall throughout the year. In areas with dense vegetation, precipitation is typically more plentiful.Because plant roots store water, soil moisture is maintained, hence soil/plant moisture content is not the main factor limiting evapotranspiration.

Precipitation is minimal in thinly vegetated places.Since soil water is difficult to store and plant water content restricts evapotranspiration generation, it is swiftly supplied after precipitation while also rapidly evaporating [45]. This study found that

ISSN PRINT 2319 1775 Online 2320 7876

 UGC CARE Listed (Group -I) Journal Volume 11, S Iss 2, 2022

evapotranspiration in arid regions has no obvious relationship with each influencing factor, and the regularity of the associated data is significantly worse. As a result, the evapotranspiration model estimation containing vegetation cover has higher potential [46–48].

The findings from the analysis of climate, environment, and geomorphology are more conclusive and can serve as a trustworthy guide for the investigation of variables influencing agriculture irrigation, drainage, and evapotranspiration [49]. Latent heat flux under various underlying surface types is determined by a variety of factors, as is the degree of correlation. The relationship between the drivers and latent heat flux is not straightforwardly linear, and under dry conditions, the effect of CO2 on latent heat flux approaches a critical level. On the research day selected for this study, the weather was sunny. Within a certain time following precipitation, the diurnal variation of ET is susceptible to observable mutation. However, the variation trend of latent heat flux under various weather conditions in June, July, and August in summer was not explored [27,51] due to the large influence of rainfall on the EC observation equipment [50]. Furthermore, there haven't been any research on latent heat flux or other climatic parameters [52].

4. Conclusions

Different underlying surface types will affect the latent heat flux distribution features when there is little fluctuation in the amount of surface plants and soil moisture.

In the same season, the diurnal variation trend of LE under various underlying surface types was statistically distinct from that of latent heat flux under the same underlying surface type.Crop midday depression influences latent heat flux when soil moisture levels are acceptable, and the change range is substantial. Low soil moisture causes a little shift in latent heat flow.

The link between temperature, CO2, and latent heat flux is significant when soil water supply is adequate. The synergistic effect of temperature and CO2 has a major impact on latent heat flow via plant transpiration and respiration when soil water availability is adequate.

In terms of time scale, all stations in the middle reaches of the Heihe River were reviewed and the relationship between influence variables and latent heat flux was examined in this study in June, July, and August 2012. As a result, more investigation

ISSN PRINT 2319 1775 Online 2320 7876

 UGC CARE Listed (Group -I) Journal Volume 11, S Iss 2, 2022

is needed to establish the function and impact of evapotranspiration in the transfer of surface energy and water circulation.

In terms of time scale, all stations in the middle reaches of the Heihe River were reviewed and the relationship between influence variables and latent heat flux was examined in this study in June, July, and August 2012. As a result, more investigation is needed to establish the function and impact of evapotranspiration in the transfer of surface energy and water circulation.

References

1. Chau, K. Use of Meta-Heuristic Techniques in Rainfall-Runoff Modelling. Water 2017, 9, 186. [CrossRef]

2. Zhang, Z.; Qin, H.; Yao, L.; Liu, Y.; Jiang, Z.; Feng, Z.; Ouyang, S. Improved Multi-objective Moth-flflame Optimization Algorithm
based on R-domination for cascade reservoirs operation. J. Hydrol. 2020, 581, 124431. [CrossRef]

3. Feng, F.; Li, X.; Yao, Y.; Liang, S.; Chen, J.; Zhao, X.; Jia, K.; Pintér, K.; McCaughey, J.H. An empirical orthogonal function-based
algorithm for estimating terrestrial latent heat flflux from eddy covariance, meteorological and satellite observations. PLoS ONE
2016, 11, e0160150. [CrossRef] [PubMed]

4. Wang, K.; Dickinson, R.E. A review of global terrestrial evapotranspiration: Observation, modeling, climatology, and climatic
variability. Rev. Geophys. 2012, 50, RG2005. [CrossRef]

5. Wang, M.; Zhang, Y.; Lu, Y.; Gong, X.; Gao, L. Detection and attribution of reference evapotranspiration change (1951–2020) in the
upper Yangtze River Basin of China. J. Water Clim. Chang. 2021, 12, 2624–2638. [CrossRef]

6. Priestley, C.H.B.; Taylor, R.J. On the Assessment of Surface Heat Flux and Evaporation Using Large-Scale Parameters. Mon.
Weather. Rev. 1972, 100, 81–92. [CrossRef]

7. Talsma, C.J.; Good, S.P.; Jimenez, C.; Martens, B.; Fisher, J.B.; Miralles, D.G.; McCabe, M.F.; Purdy, A.J. Partitioning of evapotran

ISSN PRINT 2319 1775 Online 2320 7876

 UGC CARE Listed (Group -I) Journal Volume 11, S Iss 2, 2022

spiration in remote sensing-based models. Agric. For. Meteorol. 2018, 260–261, 131–143. [CrossRef]

8. Yin, Y.; Wu, S.; Chen, G.; Dai, E. Attribution analyses of potential evapotranspiration changes in China since the 1960s. Theor.
Appl. Climatol. 2010, 101, 19–28. [CrossRef]

9. Moazenzadeh, R.; Mohammadi, B.; Shahaboddin, S.; Chau, K.-W. Coupling a fifireflfly algorithm with support vector regression to
predict evaporation in northern Iran. Eng. Appl. Comput. Fluid Mech. 2018, 12, 584–597. [CrossRef]

10. Wang, Z.; Ye, A.; Wang, L.; Liu, K.; Cheng, L. Spatial and temporal characteristics of reference evapotranspiration and its climatic
driving factors over China from 1979–2015. Agric. Water Manag. 2019, 213, 1096–1108. [CrossRef]

11. Zhang, R.; Xu, X.; Liu, M.; Zhang, Y.; Xu, C.; Yi, R.; Luo, W. Comparing evapotranspiration characteristics and environmental
controls for three agroforestry ecosystems in a subtropical humid karst area. J. Hydrol. 2018, 563, 1042–1050. [CrossRef]

12. Zhang, Y.; Kang, S.; Ward, E.J.; Ding, R.; Zhang, X.; Zheng, R. Evapotranspiration components determined by sap flflow and
microlysimetry techniques of a vineyard in northwest China: Dynamics and inflfluential factors. Agric. Water Manag. 2011, 98,
1207–1214. [CrossRef]

13. Barraza Bernadas, V.; Grings, F.; Restrepo-Coupe, N.; Huete, A. Comparison of the performance of latent heat flflux products over
southern hemisphere forest ecosystems: Estimating latent heat flflux error structure using in situ measurements and the triple
collocation method. Int. J. Remote Sens. 2018, 39, 6300–6315. [CrossRef]

14. Barraza, V.; Grings, F.; Franco, M.; Douna, V.; Entekhabi, D.; Restrepo-Coupe, N.; Huete, A.; Gassmann, M.; Roitberg, E. Estimation
of latent heat flflux using satellite land surface temperature and a variational data assimilation scheme over a eucalypt forest
savanna in Northern Australia. Agric. For. Meteorol. 2019, 268, 341–353. [CrossRef]

ISSN PRINT 2319 1775 Online 2320 7876

 UGC CARE Listed (Group -I) Journal Volume 11, S Iss 2, 2022

15. Eswar, R.; Sekhar, M.; Bhattacharya, B.K. Comparison of three remote sensing based models for the estimation of latent heat flflux
over India. Hydrol. Sci. J.-J. Des. Sci. Hydrol. 2017, 62, 2705–2719. [CrossRef]